

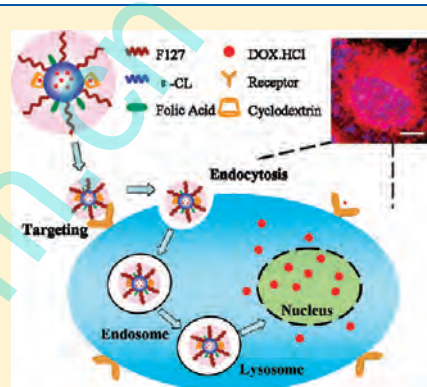
Target-Specific Cellular Uptake of Folate-Decorated Biodegradable Polymer Micelles

Qi Zhou,[†] Xing Guo,[†] Tao Chen,[†] Zhao Zhang,[†] Shijun Shao,[‡] Chao Luo,[‡] Jinrong Li,[‡] and Shaobing Zhou^{*,†,‡}

[†]Key Laboratory of Advanced Technologies of Materials, Ministry of Education, School of Materials Science and Engineering, and

[‡]School of Life Science and Engineering, Southwest Jiaotong University, Chengdu 610031, People's Republic of China

ABSTRACT: For cancer therapy, folate (FA) and β -cyclodextrin (β -CD) decorated micelles based on the biodegradable pluronic F127-*b*-poly(ϵ -caprolactone) copolymer were fabricated. These micelles were measured by dynamic light scattering measurements and atomic force microscopy. The *in vitro* release of doxorubicin hydrochloride (DOX·HCl) from the biodegradable polymer micelles was performed in a phosphate-buffered saline solution at pH 7.4 and acetate buffer solution at pH 5.0 at the temperatures of 4, 25, and 37 °C, and the results show that the release was obviously influenced by the pH and temperature. The material cytotoxicity and the tumor cell growth inhibition assays of DOX·HCl-loaded micelles were studied with the human hepatoblastoma cell line (HepG2), the lung epithelial cancer cell line (A549), and human nasopharyngeal epidermoid carcinoma cells (KB) and fibroblast normal cells using fluorescence microscopy as well as confocal laser scanning microscopy. The cellular uptake was quantitatively analyzed to further evaluate the active targeting behaviors of the micelles by flow cytometry. These quantitative and qualitative results of cellular uptake of the micelles provide evidence for the different targeting efficiencies of FA decoration for HepG2, KB, and A549 tumor cells as well as fibroblast normal cells. It also suggested that FA- and β -CD-decorated doxorubicin-loaded micelles may have great potential as nanocarriers for targeted drug delivery.



INTRODUCTION

Micelles formed from synthetic amphiphilic biodegradable block copolymers have been extensively exploited to improve conventional cancer therapy in drug delivery systems (DDSs) in recent years,^{1–5} because they could increase drug stability, drug solubility, and passive target effects due to their core–shell geometry.^{6–8} Many anticancer-drug-loaded micelles have marginal selectivity for malignant cells because they provide a tumor passive targeting by the well-known enhanced permeability and retention (EPR) effect.^{9–12}

However, these drug-loaded systems have no obvious selectivity for cell types which would also have high toxicity against normal cells.^{13,14} Targeting DDSs to a specific site selectively and quantitatively would not only improve therapeutic efficiency but also minimize negative side effects on nonpathological cells and tissues.^{15–17} Consequently, tumor-selective strategies via cellular receptors in targeted gene and drug delivery is very necessary.^{18,19} Conjugation of targeting molecules to block polymers such as folic acid (FA),²⁰ RGD peptide,²¹ mannose,²² and galactose²³ has been studied.

Among these targeted molecules, FA is a popular choice which is employed as a targeting moiety of various anticancer agents to avoid their nonspecific attacks on normal tissues as well as to increase their cellular uptake within targeted cells.^{24,25} Herein, FA was chosen as a targeting ligand since its receptors are generally overexpressed in some types of human cancers, especially ovarian, kidney, lung, brain, uterus, and colon cancer cells.²⁰

Meanwhile, hydrophobic drugs are always simply encapsulated into the hydrophobic cores in traditional polymeric micellar drug carrier systems, which would be hampered by insufficient intracellular delivery owing to the low drug loading capacity.²⁶ To overcome this shortcoming, the conjugation of hydrophilic β -cyclodextrins (β -CDs) to the polymer chains by covalent bonds may be an attractive choice. CDs have been extensively used as complexing agents to improve solubility, stability, and bioavailability of a variety of poorly soluble and labile drugs in DDSs.^{27–29} The main reason is that β -CD has a toroidal shape containing a hydrophobic inner cavity and two hydrophilic rims, and the unique structure gives CDs the capability of including a wide variety of polar and apolar “guest” molecules into their hydrophobic “host” cavity via noncovalent interactions such as hydrogen bonding, van der Waals forces, electrostatic and dipole–dipole interactions, and steric effects.^{30–33} Thus, hydrophobic anticancer drugs not only occur in the hydrophobic cores of the micelles, but also may be carried in the inner cavity of CD; that is to say, part of the drugs may appear in the hydrophilic part of the micelles.

The objective of our work was to investigate the formation of FA- and β -CD-conjugated micelles from the biodegradable pluronic F127-*b*-poly(ϵ -caprolactone) (PCL) copolymer.

Received: August 18, 2011

Revised: September 22, 2011

Published: September 26, 2011

The *in vitro* release of doxorubicin hydrochloride (DOX·HCl) from FA–F200 (F200 = PCL100–F127–PCL100) and FA–F200–CD micelles was performed in a phosphate-buffered saline (PBS) solution at pH 7.4 and acetate buffer solution (ABS) at pH 5.0 at temperatures of 4, 25, and 37 °C. The intracellular release and cell cytotoxicity of DOX·HCl-loaded micelles were studied with the human hepatoblastoma cell line (HepG2), lung epithelial cancer cell line (A549), and human nasopharyngeal epidermoid carcinoma cells (KB) and fibroblast normal cells using fluorescence microscopy as well as confocal laser scanning microscopy (CLSM). The cellular uptake efficiency was quantitatively analyzed to further evaluate the active targeting behaviors of the micelles by the fluorescence intensity from fluorescence microscopy and flow cytometry.

EXPERIMENTAL SECTION

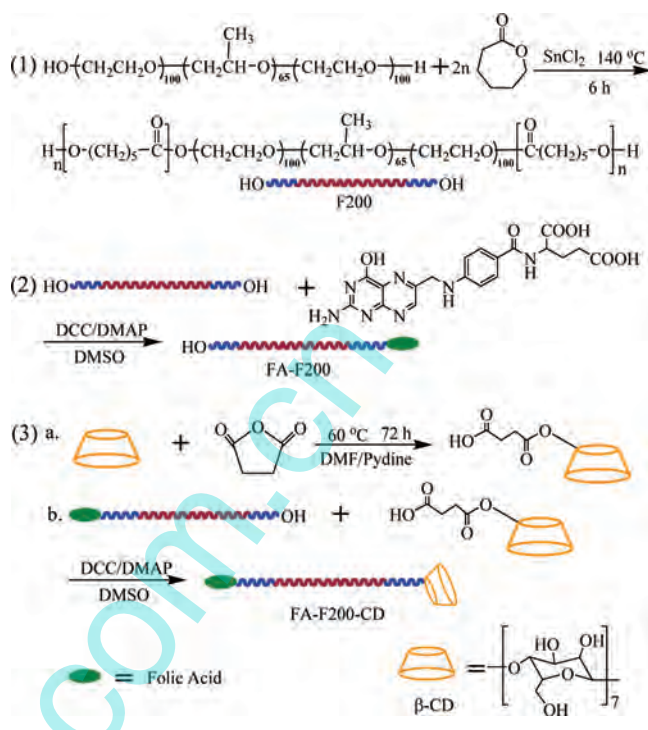
Materials. Pluronic F127 ($M_w = 12\,600$) was obtained from Aldrich and dried under high vacuum before use. ϵ -Caprolactone (ϵ -CL; Aldrich) was dried over CaH_2 for 3 days and distilled at reduced pressure prior to use. FA, β -CD, tin(II) chloride, 1,3-dicyclohexylcarbodiimide (DCC), and 4-(dimethylamino)pyridine (DMAP) were of analytical grade and used as supplied by Kelong Chemical Co. (China). Dimethyl sulfoxide (DMSO) and dimethylformamide (DMF) were purified by distillation over CaH_2 prior to use. DOX·HCl was purchased from Zhejiang Hisun Pharmaceutical Co., Ltd. (China). HepG2, A549, and KB tumor cells and fibroblast normal cells were obtained from Sichuan University (China). Other reagents were of analytical grade and used without further purification.

Synthesis of F200 Copolymers. F200 was synthesized through ring-opening polymerization (ROP) of ϵ -CL in the bulk using F127 as an initiator in the presence of SnCl_2 as the catalyst according to a previous report.³⁴ See Scheme 1. Briefly, preweighed F127 and ϵ -CL monomer were quickly added to a 50 mL round-bottom flask with a stopcock which was preheated to remove the moisture. The appropriate amount of catalyst was added to the flask. Then the flask was degassed by connecting a vacuum pump with continuous stirring to produce a well-mixed molten phase, which was carried out at 140 °C for 6 h. The obtained viscous material was dissolved with dichloromethane, precipitated in excess cold ether, and then collected by filtration. The resulting yellow product was dried in a vacuum oven before further use. The molecular weight of F200 was 20 700 obtained by gel permeation chromatography (GPC), and the characterization of F200 was introduced in our previous report.⁶

Synthesis of FA–F200. FA–F200 was synthesized as in the previous literature.³⁵ See Scheme 1. Folic acid (0.1 mmol) and DCC (0.11 mmol) were dissolved in anhydrous DMSO (10 mL). The reaction mixture was stirred overnight at room temperature. Then F200 (0.1 mmol) and DMAP (0.1 mmol) were added, and the reaction mixture was stirred at room temperature for another 24 h. The precipitated byproduct, dicyclohexylurea (DCU), was removed through centrifugation. The supernate was distilled at reduced pressure to remove DMSO and then precipitated in cold ether, filtrated, washed with pure water several times to remove the unreacted FA, and freeze-dried.

Two-Step Synthesis of FA–F200–CD. *Acidification of β -Cyclodextrin (CD-COOH).* β -Cyclodextrin was acidified just like in the acidification method of PEG as reported.³⁶ See Scheme 1. Preweighed β -cyclodextrin (0.2 mmol), succinic anhydride (SA) (0.2 mmol), and pyridine (0.1 mL) were dissolved in DMF, and

Scheme 1. Synthesis of F200, FA–F200, and FA–F200–CD Copolymers



the solution was reacted at 60 °C for 72 h. The solution was distilled at reduced pressure to dryness and then precipitated in dichloromethane to remove unreacted SA. Finally, the precipitation was dried under vacuum. The resultant product yield was 91%.

Synthesis of FA–F200–CD. CD-COOH (0.1 mmol) and DCC (0.11 mmol) were dissolved in anhydrous DMSO (10 mL). See Scheme 1. The reaction mixture was stirred overnight at room temperature. Then FA–F200 with 1 mmol of –OH groups and DMAP (0.1 mmol) were added, and the reaction mixture was stirred at room temperature for another 24 h. The precipitated byproduct, DCU, was removed through centrifugation. The supernate was distilled at reduced pressure to remove DMSO and then precipitated in cold ether, filtrated, washed with pure water several times to remove the unreacted CD-COOH, and freeze-dried. The product yield was 73%.

Characterization of Block Copolymers. Fourier transform infrared (FT-IR) spectra were obtained using a Nicolet 5700 spectrometer. KBr tablets were prepared by grinding the polymer sample with KBr and compressing the whole into a transparent tablet. ¹H NMR spectra were obtained on a Bruker AM 300 apparatus. DMSO and CDCl_3 were used as solvents. Chemical shifts are expressed in parts per million, ppm (δ). The full ultraviolet spectrum of the three kinds of micelles were also measured with a UV–vis spectrophotometer (UV-2550, Shimadzu, Japan) to confirm the graft of folic acid to F200 block polymers.

Preparation of Blank and DOX·HCl-Loaded Micelles. The blank and DOX·HCl-loaded micelle solutions were prepared by the solvent evaporation method. A typical preparation of the micelles designated as F200 is described as follows: A dry powder of 10 mg of F200 was dissolved in 5 mL of tetrahydrofuran (THF) as a good solvent, and then the solution was added dropwise using a disposable syringe (21 gauge) under high-speed stirring to 10 mL deionized water as a selective solvent.

The mixed solution was transferred to a beaker and slowly stirred at room temperature until THF was completely volatilized.

To prepare DOX·HCl-loaded micelles, 1 mg of DOX·HCl was preadded to the THF phase. The drug/polymer ratio was 1/200. After THF was completely evaporated, the drug-loaded micelles were transferred into a dialysis bag (MWCO 8000–12000) with distilled water to remove the unloaded DOX·HCl. The fabrication of the blank and drug-loaded FA–F200 and FA–F200–CD micelles underwent similar processes.

Characterization of Micelles. The critical micelle concentration (cmc) was determined using pyrene as a fluorescence probe. The concentrations of micelles from F200, FA–F200, and FA–F200–CD were varied from 5×10^{-6} to 0.1 mg/mL, and the concentration of pyrene was fixed at 0.6 μ M. The fluorescence spectra were recorded using a Fluoromax spectrometer (F-7000, Hitach, Japan) with an excitation wavelength of 390 nm. The emission fluorescences at 339 and 333 nm were monitored. The cmc was estimated as the cross-point when extrapolating the intensity ratio I_{339}/I_{333} at low and high concentration regions.

The average size, size distribution, and ζ -potential of the micelles were measured with dynamic light scattering (DLS) (Zeta-Sizer, Malvern Nano-ZS90, Malvern Ltd., Malvern, U.K.) at 25 °C. The micelle aqueous solutions (1 mg/mL) were used as the samples. Each measurement was also repeated three times, and an average value was reported.

The morphologies of the micelles were also tested by tapping-mode atomic force microscopy (AFM) measurements (CSPM5000, Beijing, China). Some droplets of micellar solution were dripped onto a clean silicon pellet and then dried at atmospheric pressure and room temperature.

The drug-loading content (DL) and encapsulation efficiency (EE) of the micelles were determined using a UV–vis spectrophotometer (UV-2550, Shimadzu, Japan). Preweighed freeze-dried DOX·HCl-loaded micelles were dissolved in 3 mL of DMSO and then were assessed by UV absorption at 488 nm.

In Vitro DOX·HCl Release from FA–F200 and FA–F200–CD Micelles. The in vitro release assay of DOX·HCl from FA–F200 and FA–F200–CD was performed in PBS solution at pH 7.4 and ABS at pH 5.0 at temperatures of 4, 25, and 37 °C. Freeze-dried drug-loaded powder was placed in a centrifuge tube and dispersed in 10 mL of PBS or ABS. The dispersed solution was incubated in a shaking water bath at 37 °C. At a predetermined time from 0.5 to 48 h, 1 mL of supernatant was taken out and replaced with the same volume of fresh medium. The concentration of DOX·HCl released was determined from the absorbance at 488 nm using a UV spectrophotometer.

In Vitro Cytotoxicity Assay. The cytotoxicity assays of the blank micelles from F200, FA–F200, and FA–F200–CD and tumor cell inhibitions of DOX·HCl-loaded micelles were evaluated using an Alamar Blue assay. HepG2, KB, and A549 were seeded into 48-well plates at 1×10^4 cells/well with 1 mL of RPMI 1640 medium, independently. After the cells were kept in the incubator at 37 °C and 5% CO₂ for 12 h, F200, FA–F200, and FA–F200–CD micelles without DOX·HCl varying from 10 to 100 μ g/mL and drug-loaded micelles with DOX·HCl varying from 0.01 to 2.5 μ g/mL were added to incubate. After 48 h, the medium was carefully removed, and 300 μ L of Alamar Blue solution (10% Alamar Blue, 80% media 199 (Gibcos), and 10% FBS, v/v) was added to each well and incubated for a further 4 h at 37 °C and 5% CO₂. A sample of 200 μ L of reduced Alamar Blue solution was pipetted into a costar opaque black-bottom 96-well plate (Sigma) and read at 570 nm (excitation)/600 nm

(emission) in an enzyme-linked immunosorbent assay (ELISA) microplate reader (Molecular Devices, Sunnyvale, CA). The results are the mean \pm standard deviation of three experiments.

Evaluation of Cellular Uptake. For qualitative cellular uptake analysis, HepG2, KB, and A549 were seeded into 12-well plates at 5×10^4 cells/well with 2 mL of RPMI 1640 medium, while fibroblast cells were seeded with α -DMEM. The cells were kept in the incubator at 37 °C in a humidified atmosphere containing 5% CO₂. After incubation for 12 h without materials, 5 μ g/mL DOX·HCl and F200, FA–F200, and FA–F200–CD micelles loaded with 5 μ g/mL DOX·HCl were added for 0.5, 3, and 6 h. After that, for CLSM (Olympus Fluoview FV1000) and fluorescence microscopy observations, the cells were fixed with 2.5% glutaraldehyde for about 20 min, and then the cell nuclei were stained with 4',6-diamidino-2-phenylindole (DAPI; blue) for 3 min. The fixed cell monolayer was finally washed three times with PBS and observed by CLSM (blue, DAPI, under excitation at 364 nm; red, DOX·HCl, under excitation at 481 nm). The fluorescence images of F200, FA–F200, and FA–F200–CD in the desired cells were also acquired by an inverted fluorescence microscope (Olympus, CKX41) with a charge-coupled device camera (Imaging, Micropublisher 5.0 RTV) and a mercury lamp (Olympus, U-RFLT50) and quantitatively analyzed using Image-Pro Plus 6.0 software. The cellular uptake efficiency is expressed as the percentage of the fluorescence intensity of the testing wells over that of the positive control wells.

To investigate the selective cellular uptake of folic-decorated micelles quantitatively, HepG2, KB, and A549 cells were incubated with F200, FA–F200, and FA–F200–CD micelles in the culture medium. To quantify the amount of doxorubicin within the cell, the cells were analyzed by flow cytometry (Epics Elite EST).

Statistical Analysis. The statistical significance of the results was analyzed using SPSS (version 16). Differences between experimental groups were compared by the Student *t* test. The results were considered statistically significant if the *p* value was less than 0.05.

RESULTS AND DISCUSSION

Characterizations of Amphiphilic F200, FA–F200, and FA–F200–CD Polymers. The chemical structures of F200, FA–F200, and FA–F200–CD were confirmed by FT-IR, ¹H NMR, and UV. As seen from FT-IR spectra in Figure 1A, a typically strong C=O stretching band appeared at 1730 cm⁻¹ in F200, which is attributed to the ester bond because of the chemical binding between F127 and ϵ -CL and among ϵ -CL monomers. The C–H stretching vibrations of PEO segments are distributed at 2975 and 2888 cm⁻¹. The peak at 1117 cm⁻¹ is ascribed to the characteristic C–O–C stretching vibration in F127. The result shows that F200 was synthesized. There is also a C=O stretching band at 1747 cm⁻¹ in CD-COOH which is not present in pure CD, which implies that part of the hydroxyl groups in CD may be modified into carboxyl groups. There are some differences in Figure 1B among the three materials. The peaks at 1418 and 1399 cm⁻¹ are attributed to the N–H stretching vibration in FA; however, it is insufficient to distinguish FA signals in FA–F200 and FA–F200–CD from those in F200. Therefore, the content of FA decorated on F200 was measured qualitatively by a UV–vis spectrum. As can be seen in Figure 1C, obvious UV absorbance peaks at about 275 nm are attributed to the aromatic ring occurring in FA–F200 and

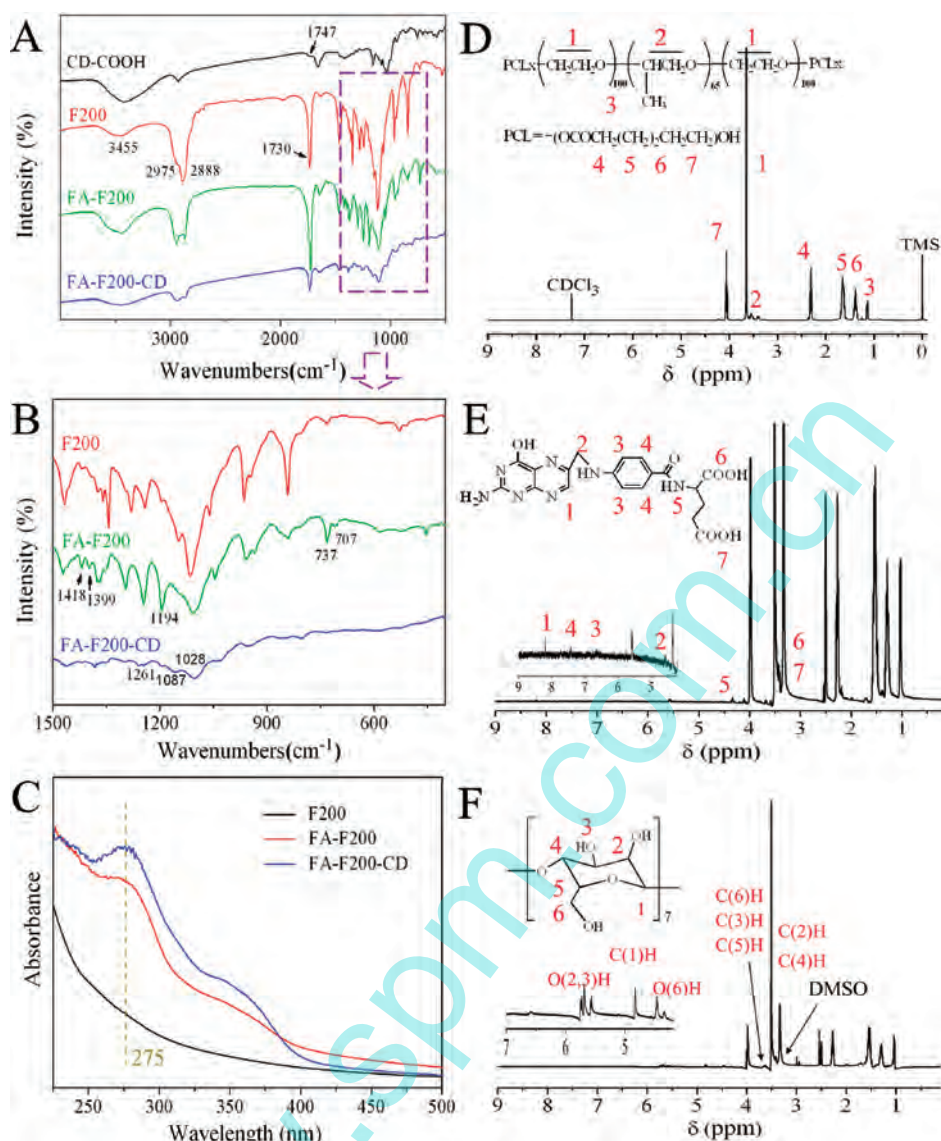


Figure 1. Characterizations of the copolymers: (A, B) FT-IR spectra of F200, FA-F200, FA-F200-CD, and CD-COOH; (C) UV-vis spectrum of the three kinds of copolymers; (D-F) ¹H NMR spectra of F200 (D) in CDCl₃ and FA-F200 (E) and FA-F200-CD (F) in DMSO-*d*₆.

FA-F200-CD.³⁷ On the basis of UV measurements, the standard curve formula was $y = 0.0803x - 0.0142$ (y axis, OD value; x axis, concentration of folic acid, mg/L). Thus, the graft ratio (mol/mol) of FA to F200 was calculated to be about 0.5:1. ¹H NMR spectra are displayed in Figure 1D,E to further confirm the formation of these polymers, which show proton peaks of F127 ($\delta = 3.62, 3.55$), CL ($\delta = 1.66, 2.33, 4.25, 6.97, \text{ and } 7.99$), FA ($\delta = 3.66, 4.34, 4.54, 5.57, 6.64, 7.41, 8.19$),¹⁷ and CD ($\delta = 3.32, 3.61, 4.46, 4.82, 5.69$).²⁸ The presence of the characteristic chemical shifts also confirmed the successful conjugation of FA and CD along the backbone of F200.

Characterizations of Micelles. To determine the cmc of these micelles, fluorescence measurements were carried out using pyrene as a fluorescent probe. The cmc values of F200, FA-F200, and FA-F200-CD are 7.57×10^{-4} , 2.46×10^{-4} , and 4.47×10^{-4} mg/mL, respectively. The improvement in hydrophilicity results in an increase of the cmc values because FA and CD are hydrophilic. The morphology of the micelles was observed by AFM. Polymeric micelles are created by a spontaneous self-assembly of

individual polymeric molecules (unimers) which are synthetic amphiphilic copolymers comprised of hydrophilic and hydrophobic blocks. It can be observed from Figure 2B that the micelles self-assembled from FA-F200-CD are all well dispersed with a regularly spherical shape. The average sizes of micelles formed from F200, FA-F200, and FA-F200-CD are 135, 132, and 123 nm, respectively, as summarized in Table 1. Both folate-free blank micelles and folate-conjugated blank micelles were negatively charged. The average ζ -potentials of F200, FA-F200, and FA-F200-CD in aqueous solution are -8.14 , -16.9 , and -15.8 mV, respectively. Changes of the ζ -potential between folate-free micelles and folate-conjugated micelles indicate that partial folate was conjugated to hydrophobic PCL exposed to the outside of the micelles. Therefore, exposure of folate realizes tumor targeting of FA-F200 and FA-F200-CD. Drug-loaded micelles slightly decreased the negativity of the micelles without significant deviation ($p > 0.05$). The drug-loading efficiencies of F200, FA-F200, and FA-F200-CD are 32.56%, 35.77%, and 58.56%, respectively. The CD decoration can obviously enhance

the drug-loading efficiency because of its hydrophobic cave, which could be a container for drug loading. Figure 2C shows the formation of typical FA–F200–CD micelles with an FA targeting molecule, which consists of an F127 corona and an ϵ -CL core. Note that the hydrophobic DOX·HCl could enter into the cavity of CD,³⁸ which is confirmed by the drug-loading efficiency. Therefore, DOX·HCl appears not only in the core of the micelle but also in its shell.

In Vitro DOX·HCl Release. Figure 3 shows that the drug release from all drug-loaded micelles exhibits a biphasic release with a burst release in the first stage followed by a period of sustained release. In Figure 3A, the initial burst release occurred in the first 3 h, which was mainly due to the release of molecules located within the hydrophilic shell, and then sustained releases occurred, indicating that DOX·HCl well-entrapped in the micelles was diffused.

Apparently, DOX·HCl releases are much faster at pH 5.0 than at pH 7.4. The accelerated DOX·HCl release in acidic pH conditions is highly desirable for effective treatment of cancer. This mainly depends on the increased solubility of DOX at acidic pH upon protonation of the glycosidic amine.³⁹ Therefore, the drug-loaded micelles prefer to release in an acid environment, and ruin of normal cells and tissues could be avoided. Temperature is another important factor that influences the release rate, and temperatures of 4, 25, and 37 °C were chosen in this study. It is interesting that the higher the temperature, the faster the drug releases. This is attributed to the fact that the solubility and

hydrophilicity of the PPO block in F127 markedly decrease with increasing temperature as a result of dehydration, which influences the micelle behaviors.³⁴

Cytotoxicity Analysis. The cytotoxicities of F200, FA–F200, and FA–F200–CD micelles are determined by quantitative evaluation of cell viability using three types of tumor cells. As shown in Figure 4, the cell viabilities of blank F200, FA–F200, and FA–F200–CD micelles exceed 100%, which indicates that the three materials are not toxic to the tumor cells under a certain concentration as high as 100 $\mu\text{g}/\text{mL}$. Then IC_{50} values were also evaluated through a coculture mixed with the cells and drug-loaded micelles after 48 h. For HepG2 cells, FA–F200–CD ($\text{IC}_{50} = 0.67 \mu\text{g}/\text{mL}$) and FA–F200 ($\text{IC}_{50} = 0.72 \mu\text{g}/\text{mL}$) exhibited superior cytotoxic activities compared to nontargeted F200 micelles ($\text{IC}_{50} = 0.92 \mu\text{g}/\text{mL}$). On the other hand, for KB cells, the IC_{50} values of FA–F200–CD ($\text{IC}_{50} = 0.89 \mu\text{g}/\text{mL}$) and FA–F200 ($\text{IC}_{50} = 0.97 \mu\text{g}/\text{mL}$) were lower than that of F200 micelles ($\text{IC}_{50} = 1.48 \mu\text{g}/\text{mL}$). Higher IC_{50} values occur for A549 cells. The IC_{50} values of F200, FA–F200, and FA–F200–CD are 2.38, 2.11, and 1.97 $\mu\text{g}/\text{mL}$, respectively. For the same cells, the IC_{50} values of the free DOX·HCl are the lowest, which would seriously damage the normal cells.

Different cells have different folate receptor (FR) expression, and then the cell uptakes are influenced.^{16,19} KB cells are known to possess much higher IC_{50} values than HepG2 because of their severe multidrug resistance (MDR) effect.¹⁶ Compared with the IC_{50} values of the three types of cells, the cell uptake increases from A549 to KB to HepG2 cells. This reveals that FA decorated onto F200 played an important role in enhancing tumor cell inhibition compared to the micelles without targeting molecules, and the introduction of CD to F200 chains can further increase the inhibition effect due to the faster drug release than FA–F200.

In Vitro Cellular Uptake of Micelles. Three tumor cell lines with different FR expressions were selected to perform the biological evaluation. Remarkably, in Figure 5A, fluorescence intensities are qualitatively obtained with an increase of the culture time from 0.5 to 6 h. The results exhibit slight DOX·HCl fluorescence for the first 0.5 h in all four cells. The fluorescence intensity of DOX·HCl inside the cells becomes very strong after 3 h and almost remains stable after 6 h for the tumor cells. In contrast, very weak fluorescence of DOX·HCl was observed for fibroblast cells treated with the same drug-loaded micelles even at 6 h. This may be attributed to the fact that there are no FRs in fibroblast cells so that there is no extra FA receptor expression between micelles and the cells. The red fluorescence occurs not only in the cytoplasm, but also in the cell nuclei. It is well-known that the growth of cancer cells cannot be effectively inhibited until DOX·HCl enters into the cell nuclei, in which the DNA of the cancer cells is broken up by DOX·HCl.^{16,19} It has been reported that the micelles are taken up by cells through a caveola-mediated endocytosis pathway.¹²

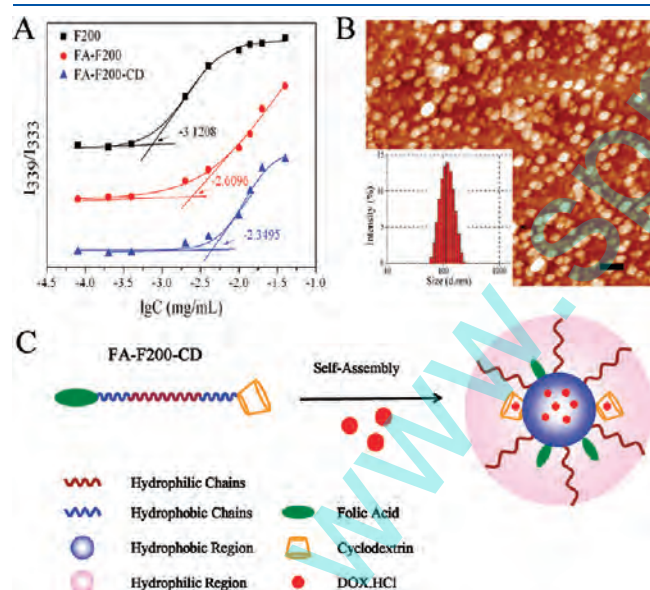


Figure 2. (A) Cmc values of the micelles from F200, FA–F200, and FA–F200–CD. (B) AFM image of FA–F200–CD (scale bar 500 nm; the inset is the size distribution of the micelles). (C) Schematic of the formation of typical FA–F200–CD micelles.

Table 1. Characterizations of F200, FA–F200, and FA–F200–CD Micelles

sample	blank micelles			DOX·HCl-loaded micelles				
	size \pm SD (nm)	PDI	ξ -potential \pm SD (mV)	size \pm SD (nm)	PDI	ξ -potential \pm SD (mV)	EE (%)	DL (%)
F200	135 \pm 5	0.163 \pm 0.068	–8.14 \pm 3.5	159 \pm 8	0.258 \pm 0.010	–9.23 \pm 5.5	32.56	0.163
FA–F200	132 \pm 5	0.158 \pm 0.113	–16.9 \pm 4.4	160 \pm 6	0.262 \pm 0.028	–18.11 \pm 4.8	35.77	0.179
FA–F200–CD	123 \pm 3	0.184 \pm 0.138	–15.8 \pm 3.2	157 \pm 7	0.356 \pm 0.013	–16.9 \pm 5.2	58.56	0.293

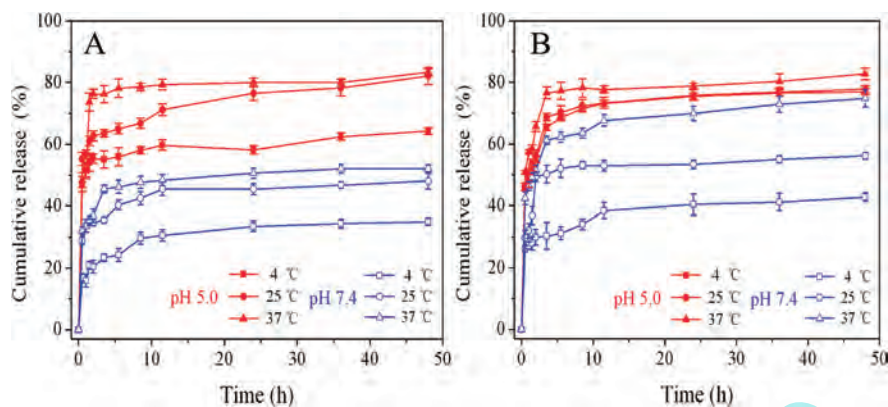


Figure 3. In vitro release profiles of DOX·HCl from drug-loaded micelles of FA-F200 (A) and FA-F200-CD (B) at pH 5.0 and 7.4 with the temperature varied from 4 to 37 °C. The standard deviation is shown by error bars that represent the mean \pm SD ($n = 3$).

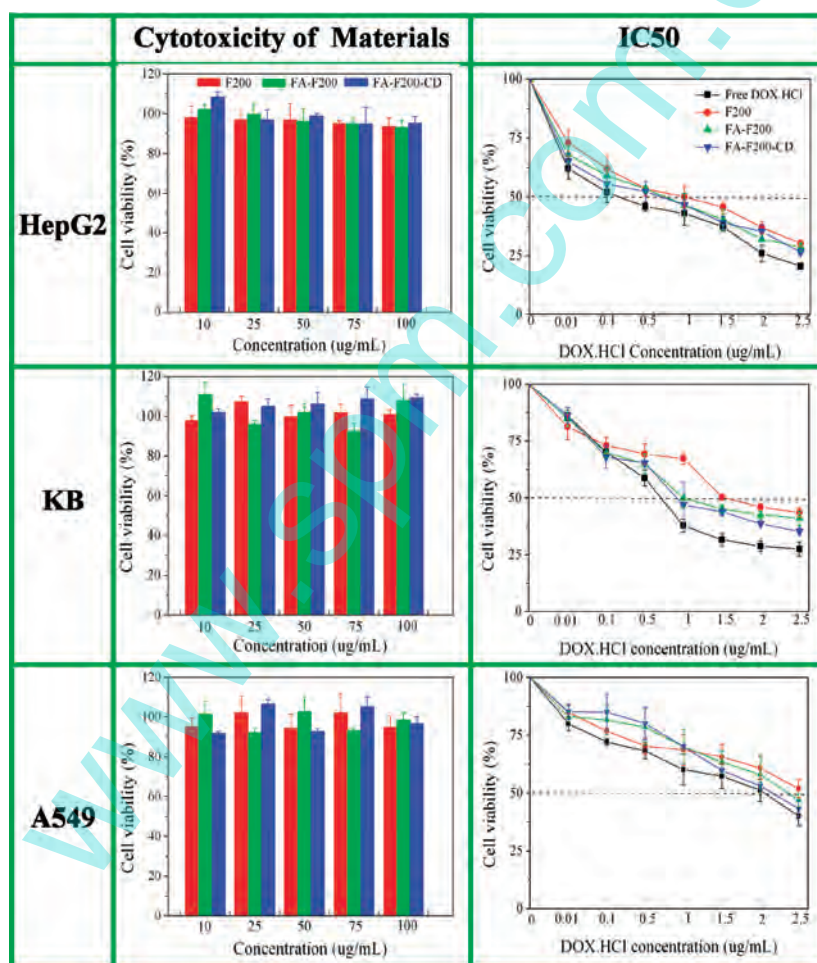


Figure 4. Cytotoxicity analysis of F200, FA-F200, and FA-F200-CD micelles in HepG2, KB, and A549 after incubation for 48 h (left) and cell viability of HepG2, KB, and A549 (right), which were exposed to different concentrations of free DOX·HCl or drug-loaded micelles for 48 h (mean \pm SD, $n = 3$).

To further analyze the degree of FA- and CD-assisted endocytosis and to better control the cancer cell uptake, a quantitative cellular uptake test was performed on the fibroblast, HepG2, KB, and A549 cells as in the previous literature.^{8,40,41} Incubation times of 0.5, 3, and 6 h were also chosen. As shown in

Figure 5B, the cell uptake efficiencies of FA-F200 and FA-F200-CD are higher than that of F200 in the cancer cells, while the uptake efficiencies almost remain the same as a function of time in the normal fibroblast cell. These results demonstrate that FA can quickly improve the endocytosis in cancer cells,

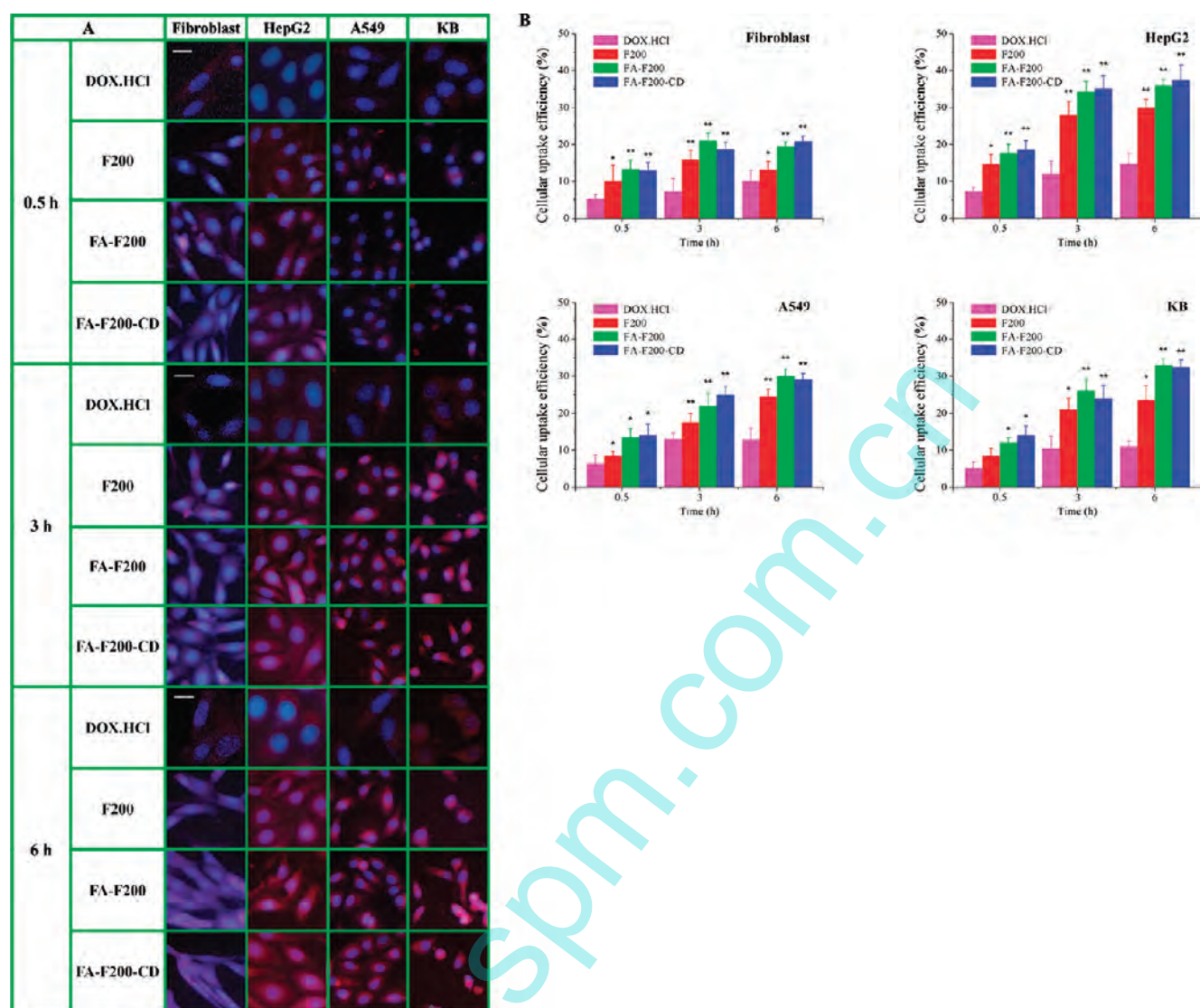


Figure 5. (A) Fluorescence microscopy images of normal fibroblast cells and HepG2, KB, and A549 tumor cells treated with DOX·HCl (red) and DOX·HCl-loaded micelles from F200, FA-F200, and FA-F200-CD for 0.5, 3, and 6 h. The scale bars are 20 μm in all the images, and cell nuclei are stained with DAPI (blue). (B) Cell uptake efficiency of normal fibroblast cells and HepG2, KB, and A549 tumor cells treated with DOX·HCl (red) and DOX·HCl-loaded micelles with 5 $\mu\text{g}/\text{mL}$ DOX·HCl from F200, FA-F200, and FA-F200-CD for 0.5, 3, and 6 h, quantitatively analyzed using Image-Pro Plus 6.0 software. Data represent the means of three repeats for each treatment (mean \pm SD; *, $p < 0.05$; **, $p < 0.01$; compared to the equivalent dose of DOX·HCl).

which could be disastrous for specific tumors with overexpressed FA receptors.

Targeting effects of micelles were also investigated by CLSM. Figure 6A shows some typical CLSM images of HepG2, KB, and A549 cells after 6 h of culture with DOX·HCl-loaded F200, FA-F200, and FA-F200-CD with 5 $\mu\text{g}/\text{mL}$ DOX·HCl at 37 $^{\circ}\text{C}$. The internalization of the fluorescent micelles and the distribution in the cells of DOX·HCl were more exactly obtained from the function of CLSM. It is noted that intracellularly transported DOX·HCl is densely located around or in the nucleus membrane and in the cell nuclei, but sparsely occurs in the cytoplasm region in the HepG2 cell. The conjugation of FA can enhance the cellular uptake from the result that the fluorescence intensities of FA-F200 and FA-F200-CD were more than that of F200. Worthy to be noted is that the fluorescence intensity of FA-F200-CD was the highest among the three

materials in HepG2 cells, which indicated that the conjugation of CD also influenced the cellular uptake efficiency because of the drug loaded into the hydrophobic cave in hydrophilic CD. It cannot be neglected that the boundaries between the nucleus cytoplasm in the KB and A549 cells were not distinct compared to that of HepG2, and the nuclei condense, which may be easily influenced by DOX·HCl because of the smaller size of the cell. These quantitative and qualitative results of cellular uptake of the micelles provide strong evidence for the targeting effect of FA decoration for HepG2, KB, and A549 cells.

Figure 6B illustrates the endocytosis of DOX·HCl-loaded FA-F200-CD micelles cultured with tumor cells. Most micelle drug delivery systems can enter into cells through caveola-mediated endocytosis.^{12,14} When FA-F200-CD micelles are cocultured with tumor cells, the micelles with a targeting ligand can band to the FA receptors around the cell membrane, and

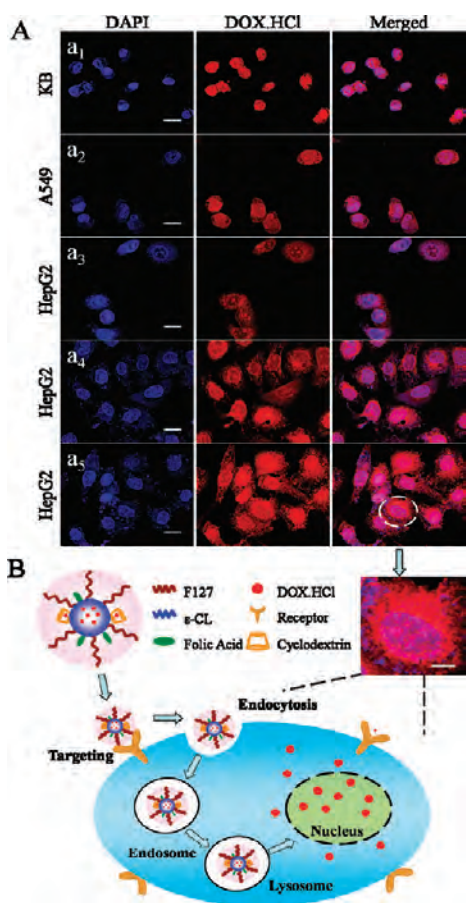


Figure 6. (A) Typical confocal microscopy images of HepG2, KB, and A549 tumor cells treated with DOX·HCl-loaded micelles from F200, FA-F200, and FA-F200-CD for 6 h. a_1 , a_2 , and a_5 belong to FA-F200-CD, and a_3 and a_4 belong to FA-F200 and FA-F200 micelles, respectively. The scale bars are $20 \mu\text{m}$ in all the images. (B) Schematic of endocytosis of DOX·HCl-loaded FA-F200-CD micelles with tumor cell targeting. The picture on the top right is the amplificatory picture of a_5 in the circle, and the scale bar is $5 \mu\text{m}$.

then the micelles are engulfed in membrane invaginations to form endosomes. After that, the endosomes deliver the drug-loaded micelles to various specialized vesicular structures toward different destinations to form lysosomes, in which the DOX·HCl-loaded micelles can release fast due to the acid pH. Finally, the DOX·HCl can diffuse around the interior of the tumor cells. The CLSM picture in the top right corner confirms that DOX·HCl can enter into the nucleolus, and then the tumor cells can be restrained.

To investigate the targeting selectivity of DOX·HCl-loaded micelles, HepG2 cells, KB cells, and A549 cells were employed as tumor cells with folic receptors. A flow cytometric analyzer was used to further quantify the folic receptor specificity of micelles targeted to the three cancer cells. Figure 7A shows the distribution of the fluorescence intensity for treatment with F200, FA-F200, and FA-F200-CD with $5 \mu\text{g/mL}$ DOX·HCl for 6 h in the three tumor cells. The results show that the mean fluorescence intensities in HepG2 cells are generally higher than those in A549 and KB, which indicates that a higher amount of DOX·HCl-loaded micelles was taken up by HepG2 than by A549 and KB cells. The result indicates that different cancer cells have different amounts of folic receptors, and HepG2 cells have the most folic receptors among the three cancer cells. The receptor cells have been fully bound by FA-decorated micelles, and the DOX·HCl-loaded micelles were transported into the cells by an FA receptor-mediated endocytosis process.

As shown in Figure 7B obtained from Figure 7A, for HepG2 cells, FA-F200 and FA-F200-CD show higher fluorescence intensities than nontargeting F200 micelles, while the intensity of FA-F200-CD is slightly lower than that of FA-F200 in spite of a higher encapsulation efficiency. On one hand, this might be attributed to the fact that DOX·HCl loaded into the hydrophobic cavity of CD prefers diffusing into the culture medium, because the CD appears in the hydrophilic region of the micelles; on the other hand, FA-F200-CD is more hydrophilic than FA-F200, which would result in quicker drug release. Therefore, the amount of endocytic delivery of DOX·HCl into cells by using FA-F200-CD micelles may actually be lower than that with FA-F200, but still higher than that with F200. The same

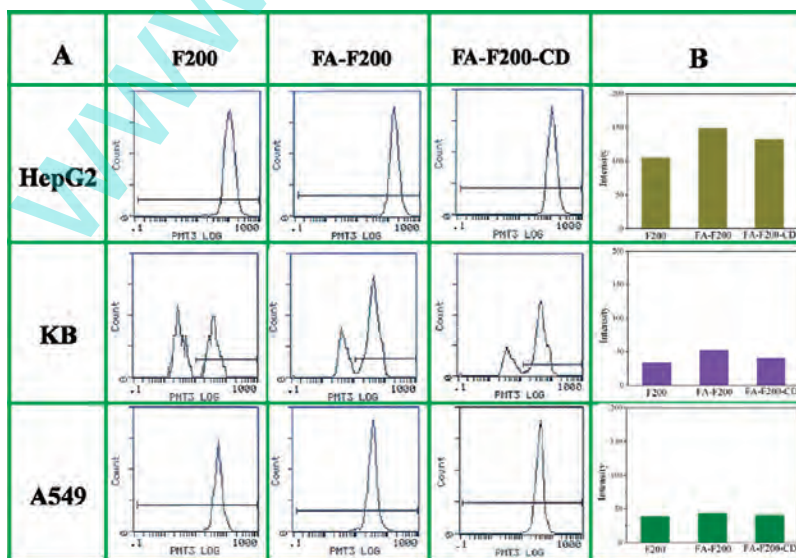


Figure 7. Flow cytometric analysis (A) and cellular uptake of the mean fluorescence intensity (B) of HepG2 cells, KB cells, and A549 cells treated with F200, FA-F200, and FA-F200-CD with $5 \mu\text{g/mL}$ DOX·HCl for 6 h.

phenomenon appears in A549 and KB cells. In summary, these results demonstrate that FA-F200 and FA-F200-CD have the ability to target HepG2, KB, and A549 cells.

CONCLUSIONS

DOX·HCl-loaded micelles with an active targeting function to tumor cells were fabricated on the basis of FA- and β -CD-decorated pluronic F127-*b*-poly(ϵ -caprolactone) copolymer. The cmc values of the micelles represent that they can retain a stable micelle structure even in a diluted environment. The in vitro release behaviors exhibit that the drug release from FA- and CD-decorated micelles is influenced by the pH and temperature. The results from in vitro cytotoxicity analysis and cellular uptake with HepG2, KB, and A549 cells demonstrate that FA-decorated micelles are of excellent biocompatibility and the DOX·HCl-loaded micelles are effective at inhibiting the growth of tumor cells. These quantitative and qualitative results of cellular uptake of the micelles provide evidence that the FA-decorated polymeric micelles possess a good active targeting effect on HepG2, KB, and A549 tumor cells with folate receptors, but no active targeting to fibroblast normal cells, and the cellular uptake efficiency can also be enhanced due to the FA-mediated targeting. Therefore, the FA- and β -CD-decorated polymeric micelles can provide a potential platform as nanocarriers in drug delivery for targeting cancer therapy.

AUTHOR INFORMATION

Corresponding Author

*Phone: 86-28-87634068. Fax: 86-28-87634649. E-mail: shaobingzhou@hotmail.com, shaobingzhou@swjtu.cn.

ACKNOWLEDGMENT

This work was partially supported by the National Natural Science Foundation of China (Grants 30970723 and 51173150).

REFERENCES

- (1) Kumar, A. P.; Depan, D.; Tomer, N. S.; Singh, R. P. *Prog. Polym. Sci.* **2009**, *34*, 479–515.
- (2) Wang, Y. P.; Xu, H. P.; Zhang, X. *Adv. Mater.* **2009**, *21*, 2849–2864.
- (3) Zhao, A. J.; Zhou, S. B.; Zhou, Q.; Chen, T. *Pharm. Res.* **2010**, *27*, 1627–1643.
- (4) Liu, T. Y.; Hu, S. H.; Liu, D. M.; Chen, S. Y.; Chen, I. W. *Nano Today* **2009**, *4*, 52–65.
- (5) Hugouvieux, V.; Monique, A. V.; Axelos, M.; Kolb, S. *Soft Matter* **2011**, *7*, 2580–2591.
- (6) Zhou, Q.; Zhang, Z.; Chen, T.; Guo, X.; Zhou, S. B. *Colloids Surf., B* **2011**, *86*, 45–57.
- (7) Ding, M.; Zhou, L.; Fu, X.; Tan, H.; Li, J.; Fu, Q. *Soft Matter* **2010**, *6*, 2087–2092.
- (8) Wang, J. F.; Liu, W. M.; Tu, Q.; Wang, J. C.; Song, N.; Zhang, Y. R.; Nie, N.; Wang, J. Y. *Biomacromolecules* **2011**, *12*, 228–234.
- (9) Farokhzad, O. C.; Langer, R. *ACS Nano* **2009**, *3*, 16–20.
- (10) Liu, G. J.; Ma, S. B.; Li, S. K.; Cheng, R.; Meng, F. H.; Liu, H. Y.; Zhong, Y. *Biomaterials* **2010**, *31*, 7575–7585.
- (11) Miao, Q. H.; Xu, D. X.; Wang, Z.; Xu, L.; Wang, T. W.; Wu, Y.; Lovejoy, D. B.; Kalinowski, D. S.; Richardson, D. R.; Nie, G. J.; Zhao, Y. L. *Biomaterials* **2010**, *31*, 7364–7375.
- (12) Sahay, G.; Alakhova, D. Y.; Kabanov, A. V. *J. Controlled Release* **2010**, *145*, 182–195.
- (13) Danhier, F.; Feron, O.; Pr at, V. *J. Controlled Release* **2010**, *148*, 135–146.
- (14) Sahay, G.; Kim, J. O.; Kabanov, A. V.; Bronich, T. K. *Biomaterials* **2010**, *31*, 923–933.
- (15) Dong, L.; Xia, S.; Wu, K.; Huang, Z.; Chen, H.; Chen, J.; Zhang, J. *Biomaterials* **2010**, *31*, 6309–6316.
- (16) Yoo, H. S.; Park, T. G. *J. Controlled Release* **2004**, *96*, 273–283.
- (17) De, P.; Gondi, S. R.; Sumerlin, B. S. *Biomacromolecules* **2008**, *9*, 1064–1070.
- (18) Bae, K. H.; Lee, Y.; Park, T. G. *Biomacromolecules* **2007**, *8*, 650–656.
- (19) Canal, F.; Vicent, M. J.; Pasut, G.; Schiavon, O. *J. Controlled Release* **2010**, *146*, 388–399.
- (20) Zhao, H.; Yung, L. Y. *Int. J. Pharm.* **2008**, *349*, 256–268.
- (21) Zhan, C. Y.; Gu, B.; Xie, C.; Li, J.; Liu, Y.; Lu, W. Y. *J. Controlled Release* **2010**, *143*, 136–142.
- (22) Wang, R.; Chen, G. T.; Du, F. S.; Li, Z. C. *Colloids Surf., B* **2011**, *85*, 56–62.
- (23) Wu, D. Q.; Lu, B.; Chang, C.; Chen, C. S.; Wang, T.; Zhang, Y. Y.; Cheng, S. X.; Jiang, X. J.; Zhang, X. Z.; Zhuo, R. X. *Biomaterials* **2009**, *30*, 1363–1371.
- (24) Kim, S. H.; Jeong, J. H.; Chun, K. W.; Park, T. G. *Langmuir* **2005**, *21*, 8852–8837.
- (25) Wang, S.; Low, P. S. *J. Controlled Release* **1998**, *53*, 39–48.
- (26) Hu, X. L.; Liu, S.; Huang, Y. B.; Chen, X. S.; Jing, X. B. *Biomacromolecules* **2010**, *11*, 2094–2102.
- (27) Dong, H. Q.; Li, Y. Y.; Cai, S. J.; Zhuo, R. X.; Zhang, X. Z.; Liu, L. *J. Angew. Chem., Int. Ed.* **2008**, *47*, 5573–5576.
- (28) Li, J.; Ni, X. P.; Zhou, Z. H.; Leong, K. W. *J. Am. Chem. Soc.* **2003**, *125*, 1788–1795.
- (29) Gou, P. F.; Zhu, W. P.; Shen, Z. Q. *Biomacromolecules* **2010**, *11*, 934–943.
- (30) Cho, S. Y.; Allcock, H. R. *Macromolecules* **2009**, *42*, 4484–4490.
- (31) Jiang, L. X.; Deng, M. L.; Wang, Y. L.; Liang, D. H.; Yan, Y.; Huang, J. B. *J. Phys. Chem. B* **2009**, *113*, 7498–7504.
- (32) Zhang, J. X.; Ma, P. X. *Angew. Chem., Int. Ed.* **2009**, *48*, 964–968.
- (33) Quan, C. Y.; J. Chen, X.; Wang, H. Y.; Li, C.; Chang, C.; Zhang, X. Z.; Zhuo, R. X. *ACS Nano* **2010**, *4*, 4211–4219.
- (34) S Kim, Y.; Ha, J. C.; Lee, Y. M. *J. Controlled Release* **2000**, *65*, 345–358.
- (35) Chen, S.; Zhang, X. Z.; Cheng, S. X.; Zhuo, R. X.; Gu, Z. W. *Biomacromolecules* **2008**, *9*, 2578–2585.
- (36) Fu, J.; Fiegel, J.; Hanes, J. *Macromolecules* **2004**, *37*, 7174–7180.
- (37) Lin, J. J.; Chen, J. S.; Huang, S. J.; Ko, J. H.; Wang, Y. M.; Chen, T. L.; Wang, L. F. *Biomaterials* **2009**, *30*, 5114–5124.
- (38) Crupi, V.; Majolino, D.; Paciaroni, A.; Stancanelli, R.; Venuti, V. *J. Phys. Chem. B* **2009**, *113*, 11032–11038.
- (39) Kim, S. Y.; Lee, K. E.; Han, S. S.; Jeong, B. *J. Phys. Chem. B* **2008**, *112*, 7420–7423.
- (40) Pan, J.; Feng, S. S. *Biomaterials* **2008**, *29*, 2663–2672.
- (41) Zhang, N.; Li, J.; Jiang, W.; Ren, C.; Li, J.; Xin, J.; Li, K. *Int. J. Pharm.* **2010**, *393*, 212–218.